0026-895X/03/6303-478–488$7.00
MOLECULAR PHARMACOLOGY
Copyright © 2003 The American Society for Pharmacology and Experimental Therapeutics
Mol Pharmacol 63:478–488, 2003

Vol. 63, No. 3
1719/1052151
Printed in U.S.A.

Differential Requirement of $G\alpha_{12}$, $G\alpha_{13}$, $G\alpha_q$, and $G\beta\gamma$ for Endothelin-1-Induced c-Jun NH_2-Terminal Kinase and Extracellular Signal-Regulated Kinase Activation

KEN ARAI, YOSHIKO MARUYAMA, MOTOHIRO NISHIDA, SHIHORI TANABE, SHUICHI TAKAGAHARA, TOHRU KOZASA, YASUO MORI, TAKU NAGAO, and HITOSHI KUROSE

Laboratory of Pharmacology and Toxicology, Graduate School of Pharmaceutical Sciences, University of Tokyo, Tokyo, Japan (K.A., Y.M., M.N., S.Tan., S.Tak., T.N., H.K.); Division of Molecular and Cellular Physiology, Center for Integrative Bioscience, National Institute for Physiological Sciences, Okazaki, Japan (M.N., Y.,M.); and Department of Pharmacology, University of Illinois at Chicago, Chicago, Illinois (T.K.)

Received March 5, 2002; accepted July 23, 2002

This article is available online at http://molpharm.aspetjournals.org

ABSTRACT

In the present study, we examined the roles of G_{12}, G_{13}, G_q, and G_i in endothelin-1-induced hypertrophic responses. Endothelin-1 stimulation activated extracellular signal-regulated kinase (ERK) and c-Jun NH_2-terminal kinase (JNK) in cultured rat neonatal myocytes. The activation of JNK, but not ERK, was inhibited by the expression of carboxyl terminal regions of $G\alpha_{12}$ and $G\alpha_{13}$. JNK activation was also inhibited by expression of the $G\alpha_{12}/G\alpha_{13}$-specific inhibitor regulator of G protein signaling (RGS) domain of p115RhoGEF and the $G\alpha_q$-specific inhibitor RGS domain of the G protein-coupled receptor kinase 2 (GRK2-RGS). JNK activation was not, however, inhibited by expression of the carboxyl terminal region of G protein-coupled receptor kinase 2 (GRK2-ct), which is a $G\beta\gamma$-sequestering polypeptide. Additionally, JNK activation but not ERK activation was inhibited by the expression of C3 exoenzyme that inactivates small GTPase Rho. These results suggest that JNK activation by $G\alpha_{12}$, $G\alpha_{13}$, and $G\alpha_q$ is involved in Rho. On the other hand, ERK activation was inhibited by pertussis toxin treatment, the receptor-G_i uncoupler, and GRK2-ct. Thus, ERK was activated by $G\alpha_i$- and $G\beta\gamma$-dependent pathways. These results clearly demonstrate that differential pathways activate JNK and ERK.

ET-1, a vasoactive peptide containing 21 amino acids, is produced by endothelial and epithelial cells, macrophages, fibroblasts, cardiomyocytes, and many other types of cells (Miyauchi and Masaki, 1999). The ET-1 receptor belongs to the superfamily of G protein-coupled receptors and consists of two subtypes, ET_A and ET_B. ET_A but not ET_B subtypes are expressed in the heart. ET-1 is involved in hypertrophic responses in vitro and in development of heart failure in vivo (Shubeita et al., 1990; Sakai et al., 1996). Although cardiac hypertrophy is assumed to be a compensatory response in its early stage, it causes myocardial infarction, arrhythmia, and sudden death. Therefore, it is important to elucidate the molecular mechanism of ET-1-induced cardiac hypertrophy. As yet, the signaling pathways leading to cardiac hypertrophy by ET-1 stimulation have not been fully examined.

To date, it is believed that ET-1-mediated responses, including MAPK activation, are mediated by $G\alpha_q$, $G\alpha_i$, and $G\beta\gamma$ (Miyauchi and Masaki, 1999). $G\alpha$ subunits are divided into four families based on homology of their amino acid sequences: G_s, G_i, G_q, and G_{12} (Simon et al., 1991). It has not, however, been determined whether the ET-1 receptor couples with G proteins other than G_q and G_i. The G_{12} family has most recently been identified and consists of two members, $G\alpha_{12}$ and $G\alpha_{13}$, which ubiquitously express throughout the body (Simon et al., 1991). It has been reported that $G\alpha_{12}/G\alpha_{13}$ are activated by stimulation of thrombin, lysophosphatidic acid, and thyroid-stimulating hormone receptors (Gohla et al., 1999). Several groups have reported that in a transient expression system that $G\alpha_{12}/G\alpha_{13}$ can regulate various intracellular effectors or cellular responses such as Na^+/H^+ exchanger (Voyno-Yasenetskaya et al., 1994), JNK (Collins et al., 1996), actin-stress fiber formation (Buhl et al., 1995; Gohla et al., 1999), apoptosis (Berestetskaya et al., 1998), and neurite retraction (Kranenburg et al., 1999). In addition,

This work was supported in part by Grant-in-Aid for Scientific Research from the Ministry of Education, Science and Culture, Japan (to T.N. and H.K.).

ABBREVIATIONS: ET-1, endothelin-1; MAPK, mitogen-activated protein kinase; ERK, extracellular signal-regulated kinase; JNK, c-Jun NH_2-terminal kinase; RGS, regulator of G protein signaling; GRK2, G protein-coupled receptor kinase 2; ct, carboxyl terminal region; PTX, pertussis toxin; MBP, myelin basic protein; HA, hemagglutinin; PCR, polymerase chain reaction; GFP, green fluorescent protein; MOI, multiplicity of infection; CHO, Chinese hamster ovary; RIPA, radioimmunoprecipitation assay; GST, glutathione *S*-transferase; PAGE, polyacrylamide gel electrophoresis; RT-PCR, reverse transcription-polymerase chain reaction; MEK, mitogen-activated protein kinase kinase; GDI, GDP dissociation inhibitor; PD98059, 2′-amino-3′-methoxyflavone; U0126, 1,4-diamino-2,3-dicyano-1,4-bis[2-aminophenylthio]butadiene.

$G\alpha_{12}/G\alpha_{13}$ can stimulate the formation of the active GTP-bound form of RhoA in cultured cells, and $G\alpha_{13}$ stimulates the GDP-GTP exchange of RhoA through the activation of Rho guanine nucleotide exchange factor in an in vitro system (Hart et al., 1998; Kranenburg et al., 1999). It is therefore possible that the ET-1 receptor couples not only with G_q and G_i but also with G_{12}/G_{13}.

G_q and G_i frequently activate MAPK, which plays an important role in cellular responses. MAPK belongs to the Ser/Thr kinase family that regulates intracellular events through phosphorylation of various proteins, including transcription factors (Widmann et al., 1999). MAPK is activated in cardiomyocytes by G protein-coupled receptors, receptor tyrosine kinases, and stress stimuli (Sugden and Clerk, 1998). There are, at least, three subfamilies of MAPK: ERK, JNK, and p38 MAPK. When these MAPKs are activated in the heart, cardiac cells turn on the reprogramming of gene expression that leads to hypertrophy. However, it has not been examined which of the G proteins or intermediate signaling proteins mediate MAPK activation by ET-1 stimulation.

To examine the contribution of each $G\alpha$ subunit to cellular responses, it is necessary to express the inhibitory proteins or peptides that show $G\alpha$ specificity. The RGS domain is a protein motif that selectively interacts with the $G\alpha$ subunits of G_q, G_i, and/or the G_{12} family (De Vries et al., 2000). The domain consists of about 120 amino acids and has been identified in at least 16 proteins. For instance, RGS4, one of the RGS proteins, interacts with $G\alpha_i$ and $G\alpha_q$ and results in inhibition of protein function by accelerating their GTPase activities (Yan et al., 1997). A further example is RGS domains of p115RhoGEF and GRK2, which show specificity toward $G\alpha_{12}/G\alpha_{13}$ and $G\alpha_q$, respectively. Therefore, this property could potentially be a powerful tool to analyze the functions of the $G\alpha$ subunits in cells.

In the present study, we investigated the roles of $G\alpha_i$, $G\alpha_q$, $G\alpha_{12}/G\alpha_{13}$, and $G\beta\gamma$ subunits on ET-1-induced JNK and ERK activation in cultured rat neonatal myocytes. Because neonatal myocytes are resistant to conventional transfection methods using calcium phosphate and polycationic lipid, we have used adenovirus gene expression system to express $G\alpha_{12}/G\alpha_{13}$- or $G\alpha_q$-specific RGS domains, carboxyl terminal regions of $G\alpha_{12}/G\alpha_{13}$ ($G\alpha_{12}$-ct/$G\alpha_{13}$-ct), and a $G\beta\gamma$-sequestering polypeptide (GRK2-ct). We demonstrate that $G\alpha_{12}/G\alpha_{13}$ and $G\alpha_q$ mediate JNK activation, whereas G_i and $G\beta\gamma$ mediate ERK activation.

Materials and Methods

Materials. ET-1 was purchased from Sigma-Aldrich (St. Louis, MO). PTX was from Calbiochem (Darmstadt, Germany). MBP, Thermoscript, and Oligo$(dT)_{20}$ primer were from Invitrogen (Carlsbad, CA). Horseradish peroxidase-conjugated anti-rabbit IgG antibody, horseradish peroxidase-conjugated anti-mouse IgG antibody, anti-JNK1 (SC-474 for immunoprecipitation), anti-JNK1 (SC-571 for Western blotting), and anti-ERK2 (SC-154 for immunoprecipitation) were purchased from Santa Cruz Biotechnology, Inc. (Santa Cruz, CA). U0126 was purchased from Funakoshi Co. (Tokyo, Japan). Rabbit anti-ERK1/2 and rabbit anti-phospho ERK1/2 antibodies (for Western blotting) were purchased from Promega (Madison, WI). Mouse anti-p38 and rabbit anti-phospho p38 antibodies were purchased from New England Biolabs (Beverly, MA). [γ-^{32}P]ATP, [^{32}P]NAD, and enhanced chemiluminescence reagent were from PerkinElmer Life Sciences (Boston, MA). Pluronic F-127 and Alexa Fluor 594 phalloidin were from Molecular Probes (Eugene, OR). The fura-2/acetoxymethyl ester was from Dojindo Laboratories (Kumamoto, Japan). Anti-HA high-affinity rat monoclonal antibody (clone 3F10) and collagenase were from Roche Diagnostics (Mannheim, Germany). RNeasy Kit was from QIAGEN (Valencia, CA). Platinum Pfx DNA polymerase and PfuTurbo DNA Polymerase were from Stratagene (La Jolla, CA). Sources of other reagents were mentioned in a previous report (Nishida et al., 2000).

Production of Recombinant Adenoviruses. $G\alpha_{12}$ and $G\alpha_{13}$ in pBluescript were provided by Dr. Melvin I. Simon (California Institute of Technology, Pasadena, CA). Rat GRK2 in pBluescript was provided by Dr. Robert J. Lefkowitz (Duke University, Durham, NC). The plasmid encoding C3 toxin was provided by Dr. Shu Narumiya (Kyoto University, Kyoto, Japan). Mouse $G\alpha_q$ was cloned from the mouse brain as follows. Total RNA was isolated from the mouse brain with RNeasy kit according to manufacturer's instruction. After reverse transcription with Thermoscript, PCR was performed by two primers: 5′-GCGCGGTACCAGAATGACTCTGGAGTCCATC-3′ (forward primer) and 5′-CGCGGATATCTTAGACCAGATTGTACTCCTT-3′ (reverse primer) for $G\alpha_q$. The amino terminal region containing the RGS domain of p115RhoGEF (p115-RGS, amino acids 1–252) was amplified with two primers 5′-GCGC GGTACCATGGAAGACTTCGCCCGAGGG-3′ (forward primer) and 5′-GCGCAAGCTTTCACAGTAGGACACAGTTCCCCATCACCTTTTTCCG-3′ (reverse primer). The extra four amino acids Cys-Val-Leu-Leu, a geranyl geranylation signal, were added at the end of the RGS domain of p115RhoGEF to facilitate translocation to the membrane. The RGS domain of GRK2 (GRK2-RGS, amino acids 1–188) was prepared by PCR with two primers: 5′-GCGCGGTACCATGGCCGACCTGGAGGCGGTA-3′ (forward primer) and 5′-CGCGAAGCTTTCACTTCCACTGGCAGAACCGTGT-3′ (reverse primer). For expression of C3 toxin, entire coding region of C3 toxin was amplified by two primers 5′-GCGCGGATCCACCATGGCTAGCTATGCAGATACTTTC-3′ (forward primer) and 5′-CGCGGTCGACAGCTATTTAAATATCATTGCTGTAATC-3′ (reverse primer). We found a sequence error at position 325 in the original sequence of C3 toxin. The correct sequence is G instead of A. Therefore, amino acid at position 109 is changed from Thr to Ala. The carboxyl terminal regions of $G\alpha_{12}$, $G\alpha_{13}$, and $G\alpha_q$ were constructed by PCR with two primers: 5′-GCGCGGTACCATGGTCCAGCGCTACCTGGTGCAG-3′ (forward primer) and 5′-CGCGCTCGAGTCACTGCAGCATGATGTCTTTCAG-3′ (reverse primer) for $G\alpha_{12}$ ($G\alpha_{12}$-ct, amino acids 325–379); 5′-GCGCGGTACCATGGTCCAAAAGTTTCTGGTGGAA-3′ (forward primer) and 5′-GCGCCTCGAGTCACTGCAGCATGAGCTGCTT-3′ (reverse primer) for $G\alpha_{13}$ ($G\alpha_{13}$-ct, amino acids 322–378); and 5′-GCGCGGTACCATGGCTCGAGAATTCATCCTGAAA-3′ (forward primer) and 5′-CGCGCTCGAGTTAGACCAGATTGTACTCCTT-3′ (reverse primer) for $G\alpha_q$ ($G\alpha_q$-ct, amino acids 305–359), respectively. All PCR products were sequenced and the identity of the sequences was confirmed. These PCR products were inserted into appropriate sites of pAdTrack-CMV. Recombinant adenoviruses encoding GFP, p115-RGS, GRK2-RGS, C3 toxin, $G\alpha_q$-ct, $G\alpha_{12}$-ct, and $G\alpha_{13}$-ct were produced by the method of He et al. (1998). Recombinant adenoviruses for expression of the carboxyl terminal region of GRK2 (GRK2-ct, amino acids 542–685) was produced as described previously (Nishida et al., 2000). Recombinant adenovirus for LacZ was provided by RIKEN DNA Bank (Tsukuba, Japan) and amplified as described previously (Nishida et al., 2000).

Cell Culture and Adenovirus Infection. Primary cultures of rat neonatal cardiomyocytes were prepared from 0 to 1 day old Sprague-Dawley rats as described previously (Nishida et al., 2000). Cardiomyocytes were plated on 2% gelatin-coated 60-mm culture dishes at density of ~7 to 8 $\times$ 10^6 cells/well (for kinase assay) or six-well plates at density of ~3 to 4 $\times$ 10^6 cells/well (for Western blot). Cells were infected by recombinant adenovirus 20 h after plating at 100 MOI (except for the infection with virus encoding GRK2-RGS, which were infected at 300 MOI). Under these conditions, almost 100% of cells expressed recombinant proteins as deter-

mined by LacZ staining or visualization of GFP. CHO-K1 cells were maintained in F-12 medium supplemented with 10% fetal bovine serum and 20 μg/ml gentamicin at 37°C. Adenovirus infection was performed at a density of $\sim 7 \times 10^4$ cells/cm^2 at 100 MOI, and the cells were cultured in F-12 medium containing 5% fetal bovine serum and 20 μg/ml gentamicin. Twenty-four hours after infection, cells were replated in slide chamber or slide glass at a density of $\sim 1 \times 10^4$ cells/cm^2. Cells were grown for additional ~12 to 16 h in the presence of fetal bovine serum, and for 24 h in the absence of fetal bovine serum before stimulation.

ERK and JNK Kinase Assays. Forty-eight hours after infection, cardiomyocytes were stimulated by ET-1 and collected by scraping in RIPA buffer (150 mM NaCl, 1.0% Nonidet P-40, 0.5% sodium deoxycholate, 0.1% SDS, and 50 mM Tris, pH 8.0) containing 2 mM EGTA, 2 mM dithiothreitol, 1 mM Na_3VO_4, 1 mM phenylmethylsulfonyl fluoride, 10 μg/ml leupeptin, and 10 μg/ml aprotinin. Cell lysates were centrifuged at 15,000 rpm at 4°C for 10 min. The supernatants were incubated with 2 μg of anti-JNK1 or 2 μg of anti-ERK2 and protein A-Sepharose for 1.5 h at 4°C. The immune complexes were washed once with RIPA buffer and then twice with kinase buffer (1 mM EGTA, 10 mM $MgCl_2$, and 50 mM Tris, pH 7.4). The immune complexes were resuspended in 40 μl of kinase buffer containing 5 μCi of [γ-^{32}P]ATP, 30 μM ATP, and 2 μg of GST-c-Jun (1–79) or 8 μg of MBP as a substrate, and then incubated for 25 min at 30°C. Reactions were terminated by the addition of SDS sample buffer and boiling for 3 min. The proteins were resolved by SDS-PAGE and radioactive bands of GST-c-Jun or MBP were quantified using filmless autoradiographic analysis (Fuji BAS1800, Fuji, Tokyo, Japan). Aliquots of supernatant of cell lysates from each sample were subjected to Western blot analysis to confirm that the equal amount of JNK or ERK was loaded in each lane.

Western Blot Analysis. Forty-eight hours after infection, cardiac myocytes were stimulated by ET-1 and collected into RIPA buffer containing 2 mM EGTA, 2 mM dithiothreitol, 1 mM Na_3VO_4, 1 mM phenylmethylsulfonyl fluoride, 10 μg/ml leupeptin, and 10 μg/ml aprotinin. After being centrifuged at 15,000 rpm for 10 min at 4°C, the supernatants were used for Western blot analysis. The samples (~20 μg) were combined with SDS sample buffer, boiled, and then subjected to SDS-PAGE followed by the transfer on to a polyvinylidene difluoride membrane by semidry method. The membrane was incubated with Tris-buffered saline-Tween 20 (20 mM Tris, pH 7.4, 137 mM NaCl, and 0.2% Tween 20) containing 5% nonfat milk, and then with anti-JNK1, anti-ERK1/2, anti-p38 MAPK, anti-phospho ERK1/2, or anti-phospho p38MAPK antibodies. The antibodies bound to the membrane were detected with horseradish peroxidase-conjugated anti-rabbit or anti-mouse IgG antibody and visualized with enhanced chemiluminescence method. Optical density on the film was measured with NIH Image. The ratios of phosphorylated ERK1/2 or p38 MAPK to total ERK1/2 or p38 MAPK were calculated, respectively. Fold stimulation was expressed by setting the control value as 1.

Intracellular Ca^{2+} Measurements of CHO-K1 Cells and Neonatal Myocytes. Fura-2 was loaded to CHO-K1 cells on coverslips by incubation in F-12 medium containing 10% fetal bovine serum, 10 μM fura-2/acetoxymethyl ester, and 0.2% (w/v) Pluonic F-127 at 37°C for 40 min, and washed with HEPES-buffered saline containing 107 mM NaCl, 6 mM KCl, 1.2 mM $MgSO_4$, 2 mM $CaCl_2$, 1.2 mM KH_2PO_4, 11.5 mM glucose, and 20 mM HEPES, adjusted to pH 7.4 with NaOH. The coverslips were then placed in a perfusion chamber mounted on the stage of the microscope. Fluorescence images of cells were recorded, and analyzed with video image analysis system (ARGUS-20/CA; Hamamatsu Photonics, Hamamatsu, Japan). The fura-2 fluorescence at an emission wavelength of 510 nm was observed at room temperature by exciting fura-2 at 340 and 380 nm. Calibration of the fluorescence signals for calculation of $[Ca^{2+}]_i$ was performed by equilibrating $[Ca^{2+}]_i$ and extracellular calcium with 5 μM ionomycin (R_{max}), followed by the addition of 10 mM EGTA (R_{min}), and by K_d value of 225 nM for fura-2 (Nishida et al., 1999). The measurement of $[Ca^{2+}]_i$ of neonatal myocytes was determined by method as described previously (Hara et al., 2002). Briefly, fura-2 was loaded to neonatal myocytes by essentially the same method as CHO-K1 cells. Pluonic F-127 was removed from HEPES-buffered saline, and the incubation time for loading fura-2 was at 37°C for 40 min. Three minutes before measuring $[Ca^{2+}]_i$, the medium was changed to Ca^{2+}-free HEPES-buffered saline containing 0.5 mM EGTA. The measurement and calibration were same as the method of CHO-K1 cells.

Detection of Gα-ct Messages by RT-PCR. Total RNA was isolated from adenovirus-overexpressed myocytes with RNeasy kit. Isolated RNA was reverse-transcribed using ThermoScript RT-PCR system and Oligo(dT)$_{20}$ primer. For subsequent verification of complete removal of genomic DNA, aliquots of each RNA sample were also subjected to mock reverse transcription, in the absence of reverse transcriptase. A cDNA was subjected to PCR for 35 cycles in a final volume of 50 μl using 1 unit of platinum Pfx DNA polymerase or PfuTurbo DNA polymerase. After an initial denaturation of 2 min at 94°C, each cycle consisted of 15 s at 94°C, 30 s at 55°C, and 40 s at 68°C. To verify removal of genomic DNA, PCR amplification was performed on the LacZ or GFP-expressed samples using the same primers. The sequences of the forward and reverse primers were 5′-GATCCGCTAGAGATCTGGTACCATG-3′ (common to $G\alpha_q$-ct, $G\alpha_{12}$-ct, and $G\alpha_{13}$-ct) and 5′-GTACTCCTTCAGGTTCAGCTGCAGG-3′ (for $G\alpha_q$-ct), 5′-CTGCAGCATGATGTCTTTCAGGTTC-3′ (for $G\alpha_{12}$-ct), or 5′-CTGCAGCATGAGCTGCTTCAGGTTG-3′ (for $G\alpha_{13}$-ct), respectively.

In Vitro PTX-Catalyzed ADP-Ribosylation of Cardiac Membrane. Cardiomyocytes pretreated with or without 100 ng/ml PTX for 18 h were washed with ice-cold phosphate-buffered saline and mechanically detached in ice-cold lysis buffer containing 50 mM Tris, pH 7.5, 5 mM EDTA, 5 mM EGTA, 10 μg/ml benzamidine, 5 μg/ml aprotinin, and 5 μg/ml leupeptin. The lysate was centrifuged at 15,000 rpm for 10 min at 4°C. The pellet was resuspended in lysis buffer with potter type homogenizer, and stored at −80°C until use. PTX was preactivated by incubation in the solution containing 50 mM Tris, pH 7.5, 5 mM ATP, 20 mM dithiothreitol, and 1 mg/ml bovine serum albumin for 30 min at 30°C. Then, activated PTX was added to assay mixture including 50 μg of the membrane prepared as described above, and incubated for 60 min at 30°C. The final concentration of all reagents in the assay mixture were as follows: 50 mM Tris, pH 7.5, 50 μM GDP, 10 mM thymidine, 5 μM NAD, 0.5 μM [^{32}P]NAD, 20 μg/ml PTX, 0.2 mg/ml bovine serum albumin, 1 mM ATP, and 4 mM dithiothreitol. The reaction was stopped by the addition of excessive amount of ice-cold 50 mM Tris, pH 7.5, and the samples were centrifuged at 15,000 rpm for 10 min at 4°C. The pellet was solubilized in SDS sample buffer, boiled, and subjected to SDS-PAGE. Radioactive bands were detected by filmless autoradiographic analysis (Fuji BAS1800).

Statistical Analysis. All data are expressed as mean ± S.E. Statistical significance was evaluated by analysis of variance, followed by Tukey's multiple range test.

Results

To examine the signaling pathways leading to JNK and ERK activation upon ET-1 stimulation, we first characterized the pattern of MAPK (ERK, JNK, and p38 MAPK) activation in cultured rat neonatal myocytes. ERK activation was observed at 30 pM and reached maximal level at around 3 nM, whereas JNK activation was observed at 0.3 nM and reached its maximally activated state at around 30 nM (Fig. 1A). The peak of ERK activation was observed after 10-min stimulation, whereas the peak of JNK activation occurred after 20-min stimulation (Fig. 1B). Therefore, ERK or JNK activation was determined by stimulation with 1 nM for 10 min or 10 nM for 20 min, respectively. From this, there is a

discrepancy in potencies between ERK and JNK activation by ET-1 stimulation, which may represent different signaling pathways leading to ERK and JNK activation. Another possible cause of the discrepancy is the different sensitivities of the two assay systems. ERK activation was determined by Western blot analysis and JNK activation was determined by phosphorylation activity. Of these, Western blot analysis may be more sensitive than phosphorylation assay analysis. In contrast to ERK and JNK activation, the extent of p38 MAPK activation by ET-1 was less than 2-fold using our detection system (data not shown). Therefore, in the present study, we did not examine further the signaling pathway of p38 MAPK activation but focused on the signaling pathways of ERK and JNK activation. We then examined the contribution of each G protein to ET-1-induced MAPK activation. To determine the involvement of G_q and G_{12}/G_{13} in ET-1-induced ERK or JNK activation, we expressed the carboxyl terminal portions of $G\alpha_q$, $G\alpha_{12}$, and $G\alpha_{13}$ ($G\alpha_q$-ct, $G\alpha_{12}$-ct, and $G\alpha_{13}$-ct) that are expected to selectively inhibit the receptor-respective G protein coupling. At first, selectivity of each $G\alpha$-ct was examined in CHO-K1 cells, because CHO-K1 cells showed a strong increase in $[Ca^{2+}]_i$ by receptor stimulation. In CHO-K1 cells, ATP stimulation increased $[Ca^{2+}]_i$ (Fig. 2A). This increase in $[Ca^{2+}]_i$ represents $G\alpha_q$-mediated phospholipase C activation and release of Ca^{2+} from intracellular storage by inositol-1,4,5-triphosphate, because $[Ca^{2+}]_i$ was determined in the absence of extracellular Ca^{2+}. The expression of $G\alpha_q$-ct but not $G\alpha_{12}$-ct and $G\alpha_{13}$-ct inhibited the ATP-induced increase in $[Ca^{2+}]_i$. This result shows that $G\alpha_q$-ct but not $G\alpha_{12}$-ct and $G\alpha_{13}$-ct selectively inhibit the ATP receptor-G_q coupling. ATP stimulation also induced actin rearrangement (Fig. 2B). In contrast to the ATP-induced increase in $[Ca^{2+}]_i$, ATP-induced actin rearrangement was inhibited by $G\alpha_{12}$-ct and $G\alpha_{13}$-ct but not $G\alpha_q$-ct. To confirm the specificity of various $G\alpha$-ct constructs in neonatal myocytes, we determined the ET-1-induced increase in $[Ca^{2+}]_i$ (Fig. 2C). ET-1 stimulation increased $[Ca^{2+}]_i$, whereas $G\alpha_q$-ct but not $G\alpha_{12}$-ct and $G\alpha_{13}$-ct inhibited an increase in $[Ca^{2+}]_i$. Because $[Ca^{2+}]_i$ was determined in the absence of extracellular Ca^{2+}, these results clearly demonstrate that $G\alpha_q$-ct selectively inhibits receptor-G_q coupling. These results also demonstrate that $G\alpha_{12}$-ct and $G\alpha_{13}$-ct selectively inhibit the signal transduction pathway of receptor-induced actin rearrangement without affecting receptor-G_q coupling. When $G\alpha_{12}$-ct or $G\alpha_{13}$-ct was expressed in neonatal myocytes, the $G\alpha$-ct constructs inhibited ET-1-induced JNK activation (Fig. 3A). JNK activation was also inhibited by $G\alpha_q$-ct (Fig. 3B). These results suggest that ET-1-induced JNK activation is mediated by G_{12}, G_{13}, and G_q. Because the $G\alpha$-ct constructs also express GFP, we compared the agonist-induced responses in GFP-expressing cells with those in LacZ-expressing cells. These results suggest that fold stimulation of ERK by agonist stimulation in GFP-expressing cells was similar to that in LacZ-expressing cells (data not shown). Because we were unable to detect respective proteins using Western blotting, we used RT-PCR methodology to detect the mRNA of $G\alpha$-ct. Expression of the $G\alpha$-ct constructs was confirmed by RT-PCR (Fig. 4). The PCR products of the $G\alpha$-ct constructs were detected only in cells infected by adenovirus coding for the respective $G\alpha$-ct sequence. The sizes of the amplified PCR products were found to agree with their predicted sizes. Therefore, it was reasonable to conclude that the $G\alpha$-ct constructs were expressed in neonatal myocytes and inhibited JNK activation. ET-1 stimulation also activated ERK, as determined by Western blot analysis using an anti-phospho-ERK antibody. In contrast to susceptibility of JNK activation to $G\alpha_{12}$-ct, $G\alpha_{13}$-ct, and $G\alpha_q$-ct, ET1-induced ERK activation was not affected by these $G\alpha$-ct constructs (Fig. 5, A and B). ERK activation was also measured by determining the ability of ERK to phosphorylate an MAPK substrate, MBP, after ERK was immunoprecipitated using an anti-ERK antibody. Although ET-1 stimulated ERK activity around 5-fold, this ERK activation was not affected by $G\alpha_{12}$-ct or $G\alpha_{13}$-ct (Fig. 6). The results obtained from measurement of MBP phosphorylation by immunoprecipitated ERK were similar to those obtained by Western blot analysis using an anti-phospho ERK antibody. Therefore, the decrease in intensity of the phosphorylated form of ERK, observed by Western blot analysis reflects the actual inhibition of ERK phosphorylating

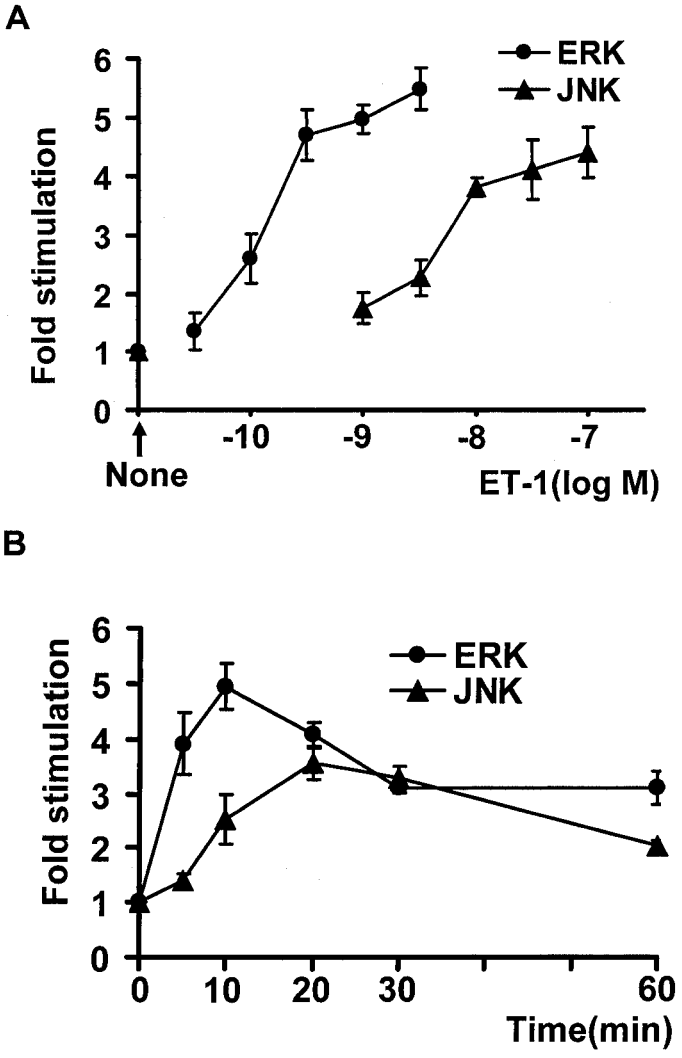

Fig. 1. Characteristics of ERK and JNK activation induced by ET-1 in cultured rat neonatal cardiomyocytes. A, dose-response curves of ERK and JNK activation induced by ET-1. Cells were stimulated by the indicated concentration of ET-1 for 10 min (ERK) or 20 min (JNK). B, time courses of ERK and JNK activation by ET-1. Cells were stimulated by 1 nM ET-1 (ERK) or 10 nM ET-1 (JNK) for the indicated time. ERK activation was determined by Western blot analysis with anti-phospho-ERK antibody, and JNK activity was determined by immune complex kinase assay as described under *Materials and Methods*. The result is shown as mean ± S.E. from three independent experiments.

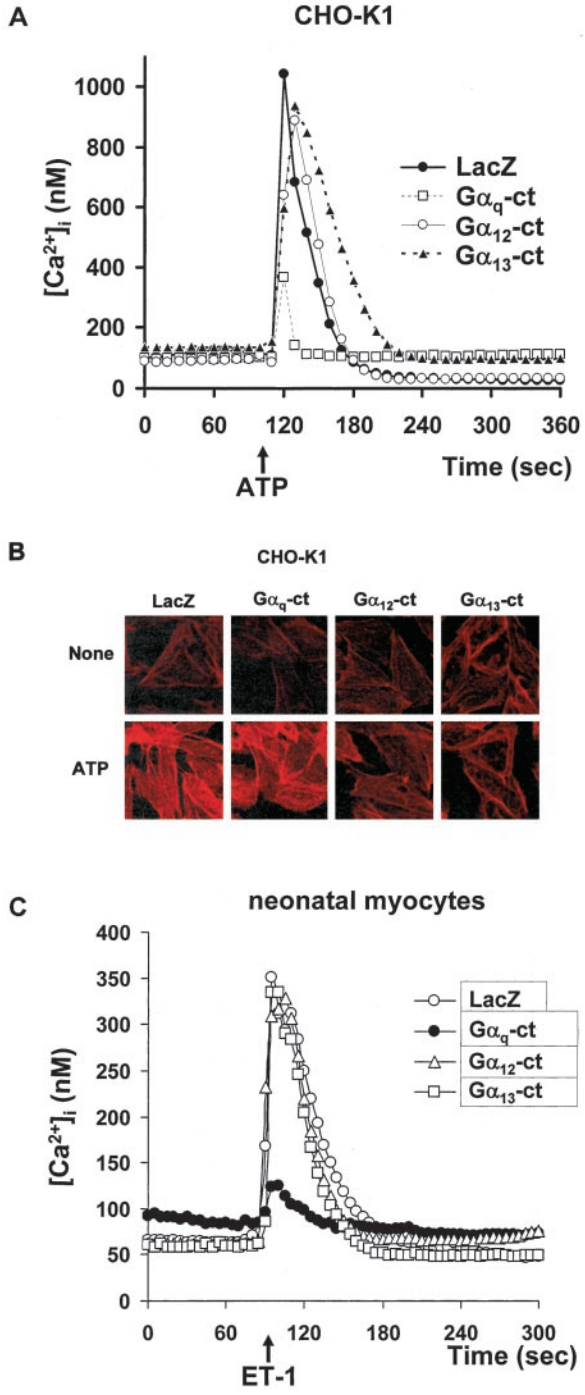

Fig. 2. Specific inhibition of each G protein signaling by respective Gα-ct constructs in CHO-K1 cells. A, effects of Gα-ct constructs on ATP-induced increase in $[Ca^{2+}]_i$. CHO-K1 cells were infected by adenoviruses coding LacZ, $G\alpha_q$-ct, $G\alpha_{12}$-ct, or $G\alpha_{13}$-ct at 100 MOI. Forty-eight hours after infection, cells were stimulated by 100 μM ATP, and $[Ca^{2+}]_i$ was measured as described under *Materials and Methods*. Typical traces of change in $[Ca^{2+}]_i$ are shown. B, effects of Gα-ct constructs on ATP-induced actin polymerization. CHO-K1 cells were infected by adenoviruses coding LacZ, $G\alpha_q$-ct, $G\alpha_{12}$-ct, or $G\alpha_{13}$-ct at 100 MOI. Sixty to 64 h after infection, cells were stimulated by 100 μM ATP for 1 h. Polymerized actin fibers were then visualized by Alexa Fluor 594 phalloidin as described under *Materials and Methods*. C, effects of Gα-ct constructs on ET-1-induced increase in $[Ca^{2+}]_i$. Neonatal myocytes were infected by adenoviruses coding LacZ, $G\alpha_q$-ct, $G\alpha_{12}$-ct, or $G\alpha_{13}$-ct at 100 MOI. Forty-eight hours after infection, cells were stimulated by 30 nM ET-1, and $[Ca^{2+}]_i$ was measured as described under *Materials and Methods*. Typical traces of change in $[Ca^{2+}]_i$ are shown.

activity. These results indicate that G_{12}, G_{13}, and G_q are involved in signaling pathway of ET-1-induced JNK activation. However, G_{12}, G_{13}, and G_q do not play any roles in ET-1-induced ERK activation.

To examine which subunits of G_{12}, G_{13}, and G_q are involved in ET-1-induced JNK activation, we constructed and

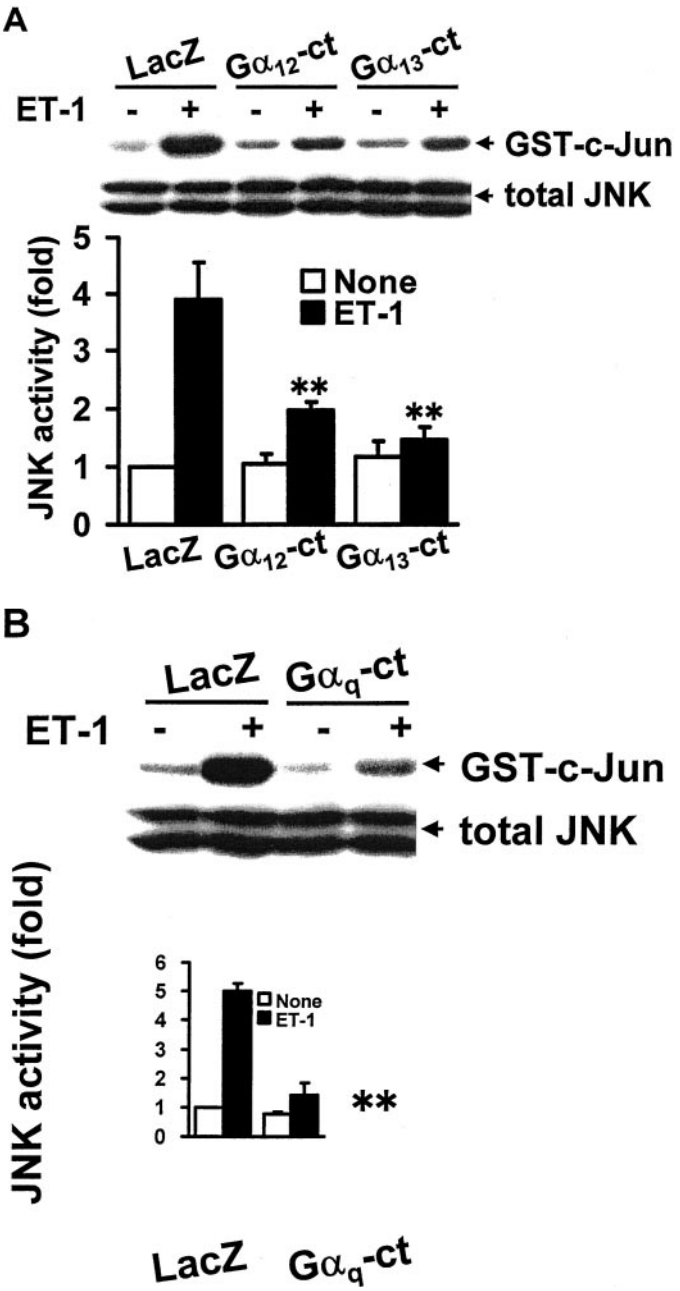

Fig. 3. Inhibitory effects of Gα-ct constructs on ET-1-induced JNK activation. Effects of $G\alpha_{12}$-ct and $G\alpha_{13}$-ct (A) and $G\alpha_q$-ct (B) on ET-1-induced JNK activation. Cells expressing LacZ, $G\alpha_{12}$-ct, $G\alpha_{13}$-ct, or $G\alpha_q$-ct were stimulated by 10 nM ET-1 for 20 min. JNK activity was determined by immune complex kinase assay using GST-c-Jun as described under *Materials and Methods*. Representative result of phosphorylation of GST-c-Jun is shown (top). JNK activity is expressed as fold increase relative to JNK activity of LacZ-expressing cells without stimulation. The result of fold increase is shown as mean ± S.E. of three independent experiments (graph). Western blot of JNK using a portion of cell lysates revealed nearly equal amounts of JNK were used for immunoprecipitation (indicated as total JNK, bottom). **, $p < 0.01$ versus ET-1 stimulation in LacZ-expressing cells.

expressed the $G\alpha_{12}$/$G\alpha_{13}$-selective RGS domain (p115-RGS), $G\alpha_q$-selective RGS domain (GRK2-RGS), and a $G\beta\gamma$-sequestering polypeptide (GRK2-ct) in neonatal myocytes. Figure 7 shows that p115-RGS almost completely inhibits ET-1-induced JNK activation (Fig. 7A) but did not affect ET-1-induced ERK activation (Fig. 7B). The expression of p115-RGS was confirmed by Western blot analysis (Fig. 7E). $G\alpha_q$-specific RGS domain GRK2-RGS inhibited JNK activation without affecting ERK activation (Fig. 7, C and D). To confirm the expression of p115-RGS and GRK2-RGS, cell lysates were subjected to Western blot analysis (Fig. 7E). p115-RGS was strongly expressed in neonatal myocytes. Because antibodies recognizing GRK2-RGS were not commercially available, we produced adenovirus for expression of HA-tagged GRK2-RGS. Western blot analysis revealed the expression of HA-tagged GRK2-RGS in neonatal myocytes and CHO-K1 cells (Fig. 7E). The expression of HA-tagged GRK2-RGS at 300 MOI was greater than at 100 MOI in the two cells. In CHO-K1 cells, GRK2-RGS at 300 MOI inhibited the increase in $[Ca^{2+}]_i$ more strongly than at 100 MOI (Fig. 7F). This result was consistent with the expression of GRK2-RGS as determined by anti-HA antibody. The inhibition by GRK2-RGS at 300 MOI was stronger than at 100 MOI, and the expression of GRK2-RGS at 300 MOI was higher than 100 MOI. Therefore, GRK2-RGS at 300 MOI inhibits the function of $G\alpha_q$ in CHO-K1 cells. The expression of GRK2-RGS in neonatal myocytes was similar to that of CHO-K1 cells. Thus, it is reasonable to conclude that GRK2-RGS at 300 MOI almost completely inhibits the function of $G\alpha_q$ in neonatal myocytes as well as in CHO-K1 cells. Thus, the higher amount (higher MOI number) of GRK2-RGS that was necessary to inhibit the JNK activation is explained by the insufficient expression of GRK2-RGS at 100 MOI. Figure 7F also shows the specificity of p115-RGS. The ATP-induced increase in $[Ca^{2+}]_i$ was not affected by the expression of p115-RGS and thus the site of action of p115-RGS is on $G\alpha_{12}$ and $G\alpha_{13}$, but not on receptor-$G\alpha$ coupling. We next determined the involvement of G_i and $G\beta\gamma$ in ET-1-induced JNK and ERK activation. In contrast to p115-RGS and GRK2-RGS, PTX treatment did not affect ET-1-induced JNK activation (Fig. 8A). However, PTX treatment did inhibit ERK activation (Fig. 8B). An MEK inhibitor, U0126, almost completely inhibited ERK activation as expected (Fig. 8B). The inability of PTX to affect JNK activation was not due to inefficient ADP-ribosylation of $G\alpha_i$ but the prior PTX treatment did abolish in vitro ADP-ribosylation of the membranes (Fig. 8C). Therefore, PTX treatment abolished the function of endogenous $G\alpha_i$ under the present experimental conditions. PTX treatment and GRK-ct inhibited ERK activation but $G\alpha_q$-ct, $G\alpha_{12}$-ct, and $G\alpha_{13}$-ct did not inhibit the activation. The ET-1-induced activation of ERK is therefore mainly regulated by $G\beta\gamma$ of G_i. To examine whether inhibition of ERK detected by Western blotting reflected the inhibition of ERK activity, we

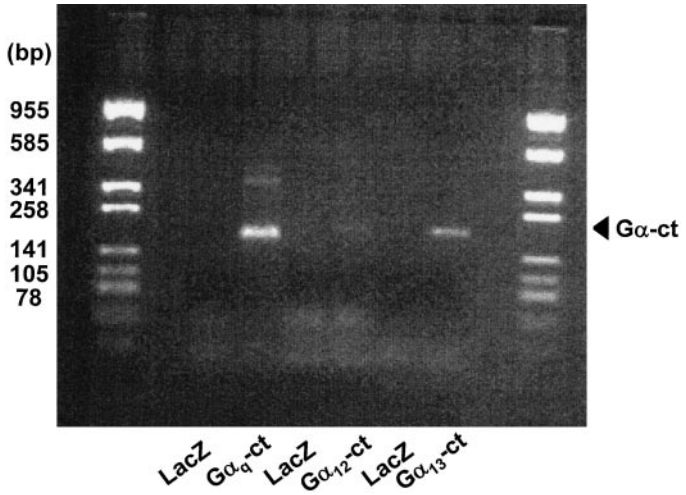

Fig. 4. RT-PCR of various Gα-ct constructs. Total RNA was prepared from cells infecting with LacZ, $G\alpha_{12}$-ct, $G\alpha_{13}$-ct, or $G\alpha_q$-ct-expressing adenoviruses. After reverse transcription, PCR was performed with two primers: one is derived from vector region and the other is from the carboxyl terminal sequence that is specific for each Gα. PCR products were run on 2.0% agarose gel.

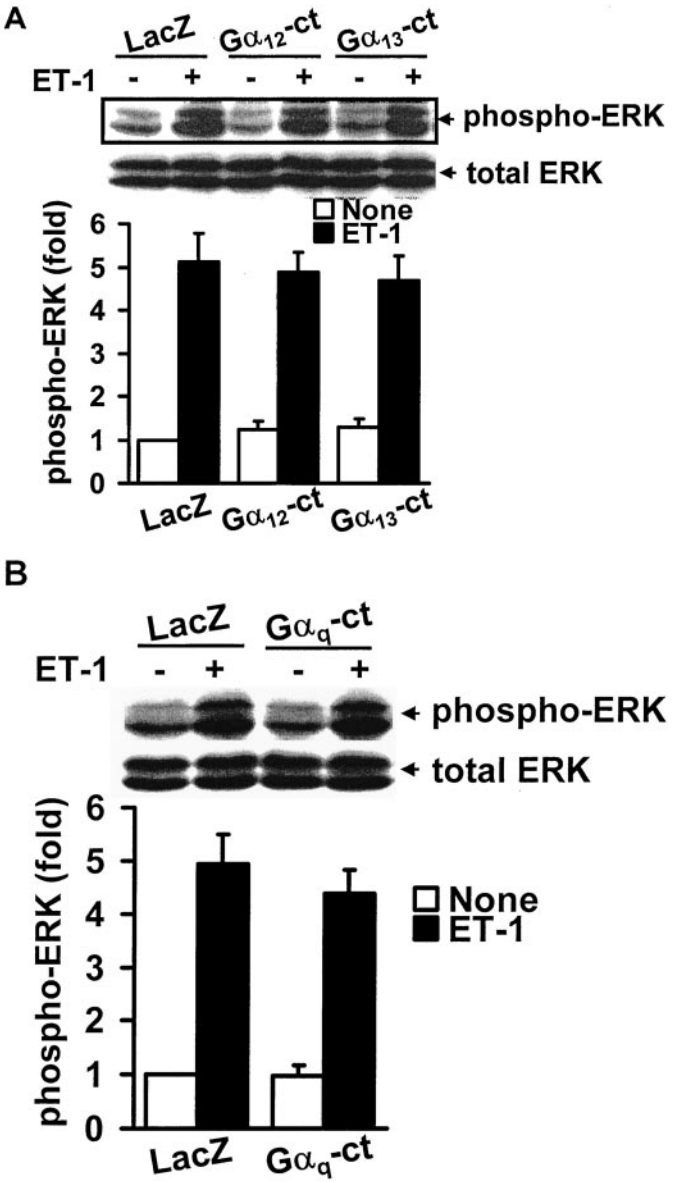

Fig. 5. Effects of Gα-ct constructs on ET-1-induced ERK activation as determined by Western blot analysis with anti-phospho ERK antibody. Cells expressing $G\alpha_{12}$-ct, $G\alpha_{13}$-ct (A), or $G\alpha_q$-ct (B) were stimulated by 1 nM ET-1 for 10 min, and ERK activation was determined by Western blot as described under *Materials and Methods*. Typical result of ERK activation by Western blot analysis is shown (top). The result of fold increase is shown as mean ± S.E. of at least three independent experiments (graph).

determined ERK activity in an immunocomplex. From this, ET-1 stimulation increased ERK activity by about 5-fold (Fig. 9A). This activation was inhibited by GRK2-ct and PTX treatment (Fig. 9, A and B). The ET-1-induced increase in ERK phosphorylating activity was also inhibited by the MEK inhibitor U0126, indicating that ERK is activated by MEK (Fig. 9B). Therefore, the inhibition of ERK detected by Western blot analysis actually reflects the inhibition of ERK activity.

It has been reported that G_{12} and G_{13} regulate the Rho-dependent signaling pathway. To investigate this, we examined the role of Rho in ET-1-induced JNK and ERK activation. The C3 toxin, which was expressed in neonatal myocytes to inactivate Rho, almost completely inhibited JNK activation without affecting ERK activation (Fig. 10, A and B). Rho may be located downstream of $G\alpha_{12}$, $G\alpha_{13}$, and $G\alpha_q$, and lead to activation of JNK but not ERK.

Discussion

One of the aims in the present study was to examine whether G_{12} and G_{13} are involved in ET-1-induced MAPK activation. No previous reports have directly demonstrated the coupling of the ET-1 receptor with G_{12} and/or G_{13}. To examine the contribution of G_{12} and G_{13} to ET-1-mediated signal transduction pathways, we developed two types of reagent. One of the reagents was a carboxyl terminal portion of $G\alpha_{12}$ and $G\alpha_{13}$ that interferes with the receptor G protein coupling. The carboxyl terminal portion of $G\alpha$ is important for the coupling of receptors with G proteins (Hamm, 1998). Three groups have demonstrated that the carboxyl terminal portion of $G\alpha$ can block receptor-mediated G protein activation in cells. Gilchrist et al. (2001) reported that 11 amino acid peptides derived from carboxyl terminal portions of $G\alpha_q$ but not $G\alpha_i$ inhibit thrombin-mediated $[Ca^{2+}]_i$ flux in endothelial cells. Akhter et al. (1998) reported that carboxyl terminal polypeptide of $G\alpha_q$ consisting of 55 amino acids, inhibits α_1-adrenergic receptor-induced inositol phosphates accumulation in vitro and blocks hypertrophy induced by pressure overload in vivo. Yuan et al. (2001) reported that the fusion protein of GFP with a carboxyl terminal of 45 amino acids of $G\alpha_{13}$ inhibits bombesin-induced protein kinase D activation (Yuan et al., 2001). We demonstrated in the present study the selectivity of various $G\alpha$-ct constructs to inhibit the coupling of $G\alpha$ with receptor. The results demonstrated that various $G\alpha$-ct constructs could be used for analyzing the role of G proteins in receptor-mediated G protein signaling.

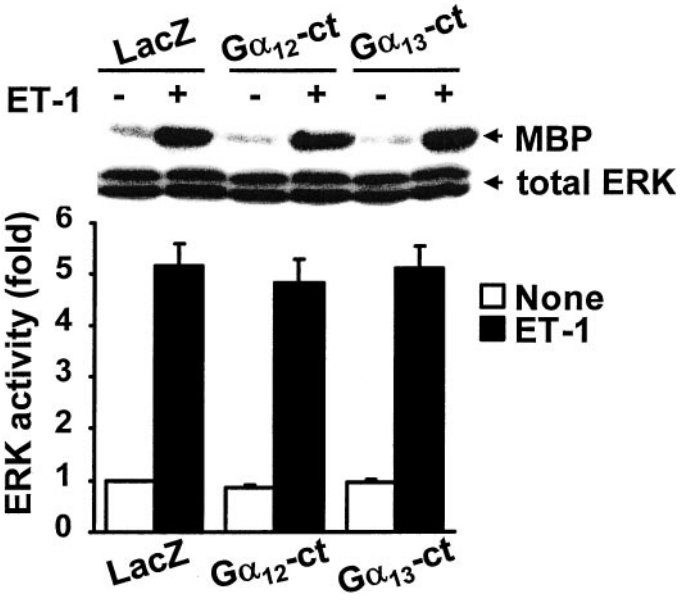

Fig. 6. Effects of $G\alpha_{12}$-ct and $G\alpha_{13}$-ct on ET-1-induced ERK activation as determined by phosphorylation activity. Cells expressing LacZ, $G\alpha_{12}$-ct, or $G\alpha_{13}$-ct were stimulated by 10 nM ET-1 for 10 min. Cell extract was prepared and subjected to immunoprecipitation by anti-ERK2 antibody. ERK activity in immune complex was then determined using MBP as a substrate. Representative result of kinase assay is shown (top). ERK activity is expressed as fold increase relative to the activity of unstimulated LacZ-expressing cells. The result of fold increase is shown as mean ± S.E. of three independent experiments (graph). Western blot of ERK using a portion of cell lysates revealed nearly equal amounts of ERK were used for immunoprecipitation (bottom).

Another reagent is a polypeptide coding RGS domain that selectively interacts with $G\alpha_q$ or $G\alpha_{12}/G\alpha_{13}$. The RGS domain is defined as a region of about 120 amino acids and has been identified in at least 16 different protein species. Many of these interact with $G\alpha_i$ or $G\alpha_q$ and accelerate their GTPase activities. The RGS domains specific for $G\alpha_q$ and $G\alpha_{12}/G\alpha_{13}$ have been recently identified in GRK2 and p115RhoGEF, respectively (Hart et al., 1998; Kozasa et al., 1998; Carman et al., 1999). Rümenapp et al. (2001) reported that the expression of the RGS domain (Lsc-RGS) of mouse homolog of p115RhoGEF in human embryonic kidney 293 cells inhibits muscarinic acetylcholine receptor-mediated phospholipase D activation and is regulated by $G\alpha_{12}/G\alpha_{13}$ but not $G\alpha_q$. We have demonstrated in the present study that the RGS domain of p115RhoGEF in cultured rat neonatal myocytes almost completely inhibits JNK activation without significantly affecting ERK activation. The present results observed with $G\alpha$-ct constructs and RGS domains strongly support the belief that ET-1 receptor couples with G_{12}/G_{13}, and α subunits of G_{12}/G_{13} are involved in ET-1-induced JNK activation. So far, there are no convenient reagents that selectively block the functions of PTX-insensitive $G\alpha$ subunits such as $G\alpha_q$ and $G\alpha_{12}/G\alpha_{13}$. These present results, together with the Rümenapp et al. (2001) results, demonstrate that RGS domains are selective for PTX-insensitive $G\alpha_q$ and $G\alpha_{12}/G\alpha_{13}$ and powerful tools to dissect their functions in cells.

It may be thought that various $G\alpha$-ct constructs should inhibit all kinds of receptor-G protein coupling, irrespective of the origin of carboxyl terminal sequences, because their site of action is a receptor-G protein interface. However, two reports suggest that the receptor exists in several different conformations (MacKinnon et al., 2001; Vilardaga et al., 2001). Vilardaga et al. (2001) reported that parathyroid hormone receptor mutants, with an impaired ability to couple with G_q, do not show reduced responses to agonist-mediated phosphorylation of the receptor by GRK2, nor agonist-induced recruitment of β-arrestin to the cell membrane (Vilardaga et al., 2001). MacKinnon et al. (2001) reported that a substance P analog binds to the ligand-binding site shared by bombesin, and the substance P analog and bombesin activate the JNK and ERK. Although a dominant negative mutant of $G\alpha_{12}$ blocked JNK and ERK activation induced by these two agonists, ERK activation by the analog but not bombesin was PTX-sensitive (MacKinnon et al., 2001). These results indicate that the receptor exists in several conformations that are differentially recognized by dif-

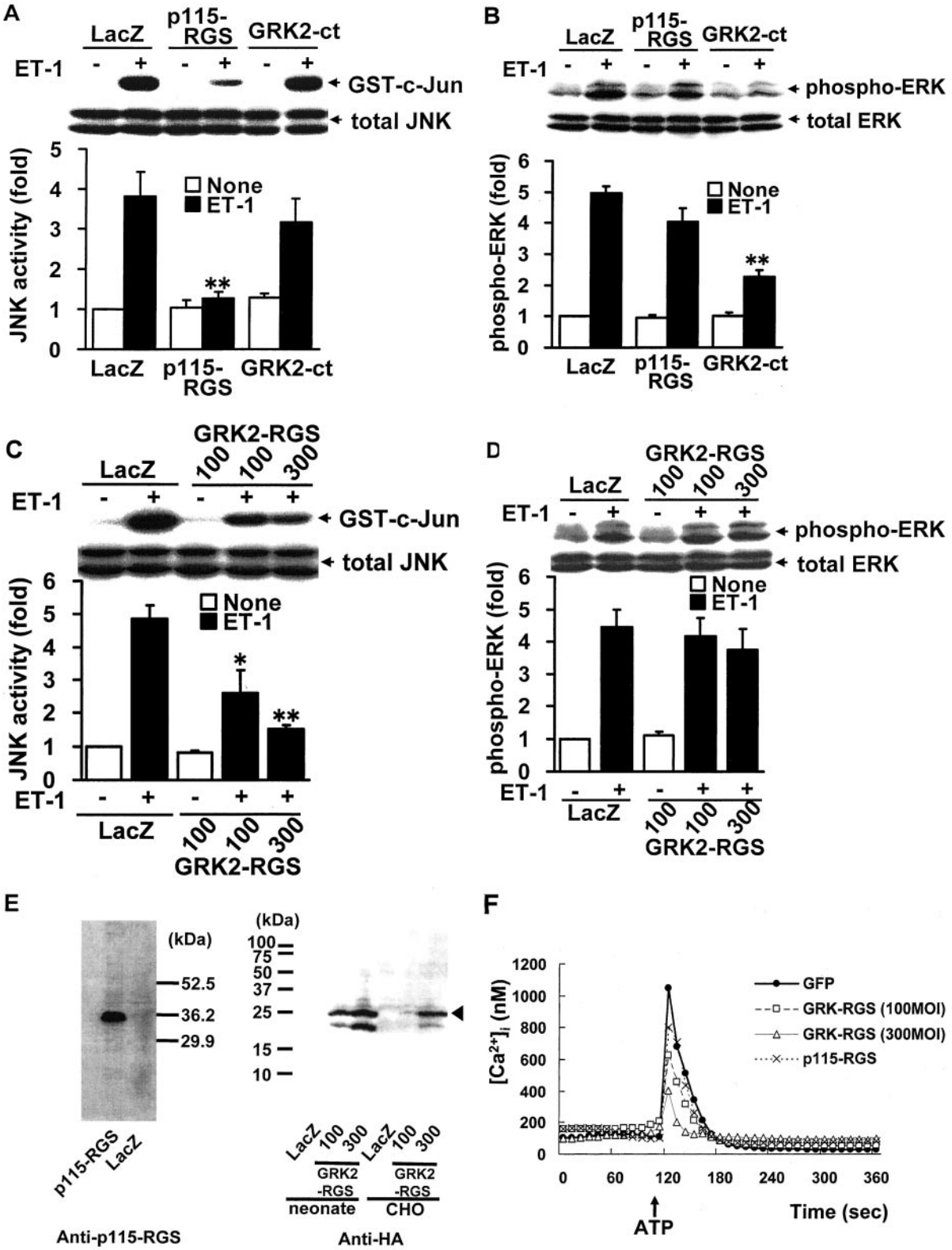

Fig. 7. Determination of G protein species involved in ET-1-induced 1 nM ET-1 for 10 min (ERK) or JNK and ERK activation. A to D, cells were infected by adenoviruses coding p115-RGS or GRK2-ct or GRK2-RGS. These cells were stimulated by 10 nM ET-1 for 20 min (JNK). JNK activity (A and C) was determined by immune complex kinase assay as described under *Materials and Methods*. ERK activation (B and D) was determined by phospho-ERK specific antibody. Representative results of kinase assay or Western blot are shown (top). JNK activity and ERK activation were expressed as fold increase relative to those of unstimulated LacZ-expressing cells. The result of fold increase is shown as mean ± S.E. of at least three independent experiments (graph). $*$ or $**$, $p < 0.05$ or $p < 0.01$ versus ET-1 stimulation of LacZ-expressing cells, respectively. E, expression of p115-RGS or GRK2-RGS was determined by Western blot analysis. Cells were infected by adenoviruses expressing p115-RGS or HA-tagged GRK2-RGS with MOI of 100 or 300. The cell lysates were used for Western blot analysis with polyclonal anti-p115-RGS or monoclonal anti-HA antibody. F, effects of p115-RGS and GRK2-RGS on the ATP-induced increase in $[Ca^{2+}]_i$. CHO-K1 cells were infected by adenoviruses coding GFP, GRK2-RGS or p115-RGS at 100 or 300 MOI. Forty-eight hours after infection, cells were stimulated by 100 μM ATP, and $[Ca^{2+}]_i$ was measured as described under *Materials and Methods*. Typical traces of change in $[Ca^{2+}]_i$ are shown.

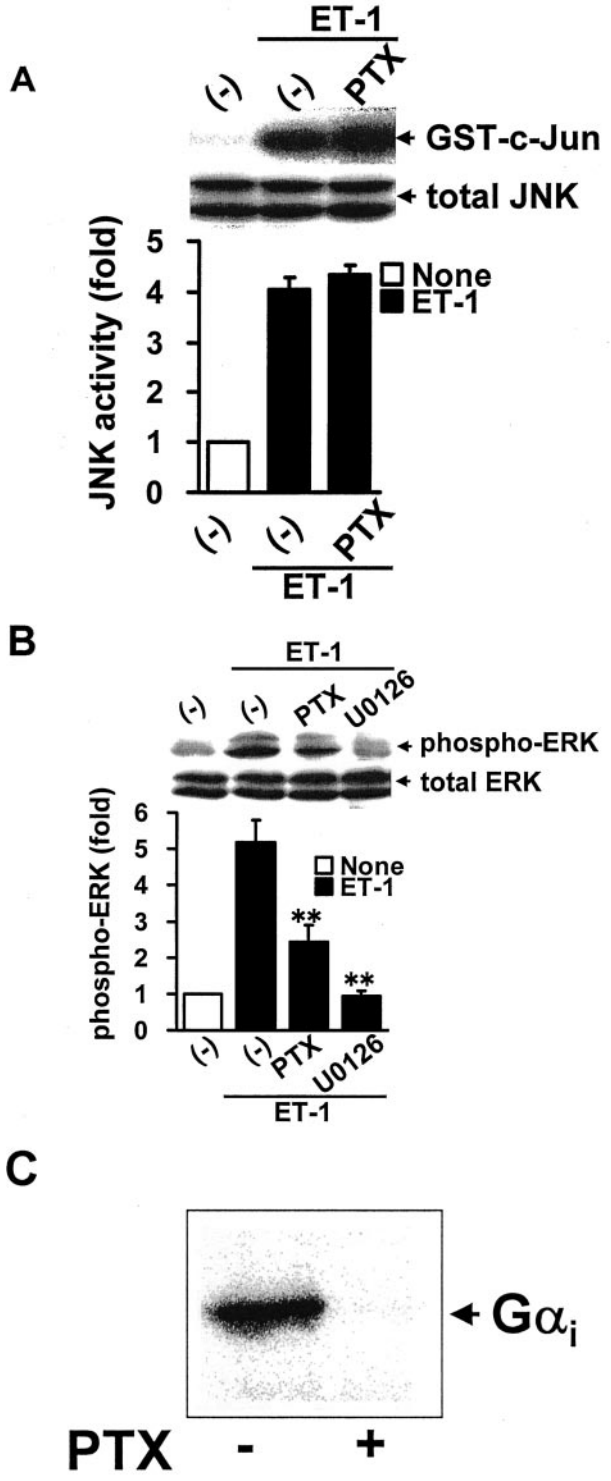

Fig. 8. Effect of PTX or MEK inhibitor U0126 on ET-1-induced JNK and ERK activation. Cells were pretreated with PTX (100 ng/ml; 18 h) or U0126 (10 μM, 30 min) and stimulated by 1 nM ET-1 for 10 min (ERK) or 10 nM ET-1 for 20 min (JNK). A, JNK activity was determined by immune complex kinase assay using GST-c-Jun as described *Materials and Methods*. Representative result of phosphorylation of GST-c-Jun is shown (top). B, ERK activation was determined by Western blot analysis. Representative result of Western blot analysis is shown (top). Pretreatment with PTX or U0126 alone did not affect basal ERK activation state (data not shown). The result is shown as mean ± S.E. of at least three experiments (graph). **, $p < 0.01$ versus ET-1 stimulation of LacZ-expressing cells. C, ADP-ribosylation of $G\alpha_i$ by PTX was performed using membrane fractions prepared from PTX-untreated (−) or treated (+) cells as described under *Materials and Methods*.

ferent signaling proteins. Therefore, it is possible that $G\alpha_q$ and $G\alpha_{12}/G\alpha_{13}$ interact with the ET-1 receptor in a different conformation. If so, $G\alpha_{12}$-ct and $G\alpha_{13}$-ct do not interfere with the receptor-G_q coupling, and $G\alpha_q$-ct does not affect receptor-G_{12}/G_{13} coupling.

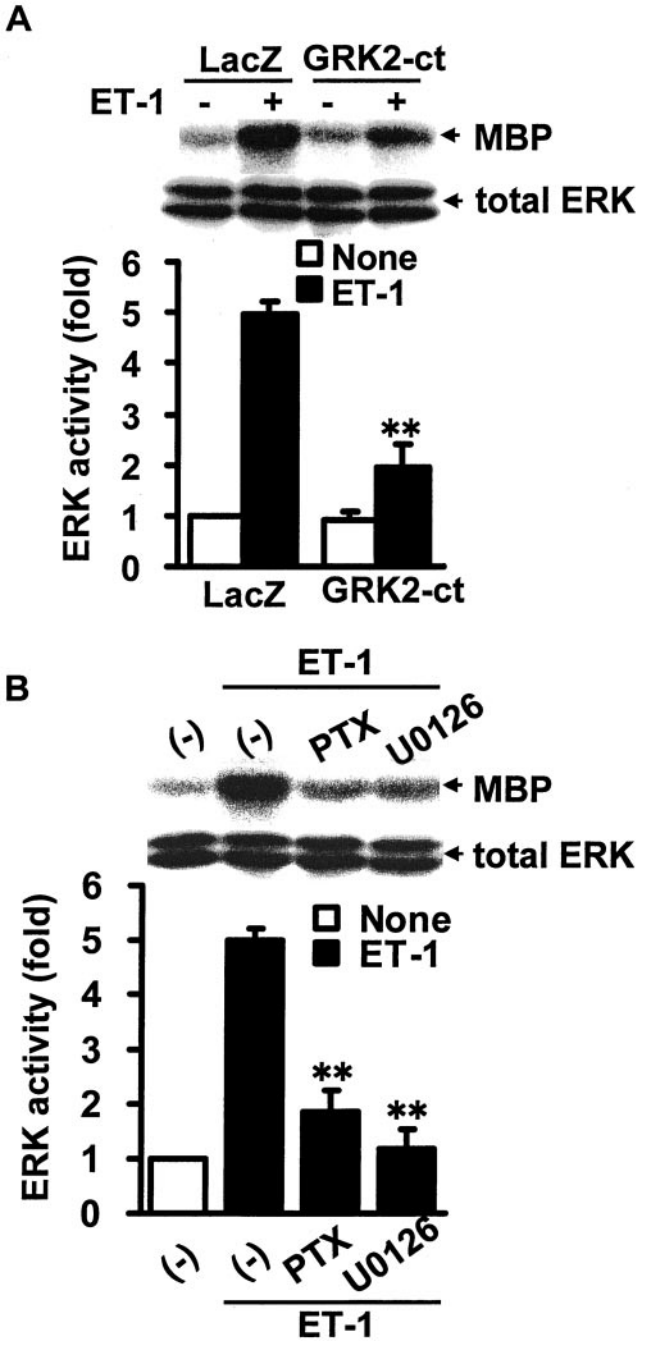

Fig. 9. Involvement of $G\beta\gamma$ and G_i in ET-1-induced ERK activation. Cells expressing GRK2-ct (A) or pretreating with 100 ng/ml PTX for 18 h or 10 μM U0126 for 30 min (B) were stimulated by 10 nM ET-1 for 10 min. Cell lysate was prepared and subjected to immunoprecipitation with anti-ERK2 antibody, and immune complex kinase assay with MBP as a substrate were performed as described under *Materials and Methods*. Representative result of kinase assay is shown (top). ERK activity was expressed as fold increase relative to that of unstimulated LacZ-expressing cells. The result is shown as mean ± S.E. of three independent experiments (graph). Western blot of ERK using a portion of cell lysates revealed nearly equal amounts of ERK were used for immunoprecipitation (bottom). **, $p < 0.01$ versus ET-1 stimulation of LacZ-expressing cells.

It has been reported that Rho is involved in cardiac hypertrophy. Transfection or infection of constitutively active RhoA stimulates atrial natriuretic factor expression (Sah et al., 1996; Thorburn et al., 1997; Hoshijima et al., 1998) and myofibrillogenesis (Thorburn et al., 1997; Hoshijima et al., 1998). On the other hand, dominant negative RhoA prevents phenylephrine-induced (Sah et al., 1996), G_q-stimulated (Hines and Thorburn, 1998), and Ras-induced (Thorburn et al., 1997) hypertrophy. Considering these reports, we examined whether Rho is involved in ET-1-induced MAPK activation. To ablate the function of Rho, we expressed the C3 toxin in neonatal myocytes using the adenovirus gene expression system. The C3 toxin inactivates Rho by ADP-ribosylation of Asn^{41} in its effector domain. The present study demonstrated that the C3 toxin almost completely inhibited ET-1-induced JNK but not ERK activation. Because $G\alpha_{12}$-ct and $G\alpha_{13}$-ct inhibited JNK activation, and $G\alpha_{13}$ activates RhoA via p115-RhoGEF in vitro (Hart et al., 1998), it is reasonable to conclude that $G\alpha_{12}$ and $G\alpha_{13}$ activate JNK through Rho. The present study also showed that $G\alpha_q$-ct as well as $G\alpha_{12}$-ct and $G\alpha_{13}$-ct inhibited JNK activation. Although cross talk between $G\alpha_q$- and $G\alpha_{12}/G\alpha_{13}$-signaling pathways is unknown, a recent report suggests that the activation step of Rho is a site of $G\alpha_q$ action (Mehta et al., 2001). Rho locates in the cytosol as a complex with GDI. Rho should dissociate from GDI before Rho is translocated to the membrane and activated by receptor stimulation. The report demonstrated that the protein kinase C-α phosphorylates GDI of the Rho-GDI complex, and the resulting phosphorylation of GDI leads to dissociation of the complex into Rho and GDI (Mehta et al., 2001). Thus, $G\alpha_q$ may be involved in phosphorylation of GDI through activation of protein kinase C-α. It remains to be determined whether $G\alpha_q$ contributes to Rho activation in neonatal myocytes.

In conclusion, the present study demonstrates for the first time that $G\alpha_{12}$, $G\alpha_{13}$, and $G\alpha_q$ are involved in ET-1-induced JNK activation in cells. We also demonstrate that ERK activation by ET-1 stimulation is mediated by G_i and $G\beta\gamma$. Further investigations to analyze the functions of $G\alpha_q$, $G\alpha_{12}$, and $G\alpha_{13}$ in in vivo animal model will provide an interesting insight into the physiological meaning of ET-1-mediated JNK activation through $G\alpha_{12}$, $G\alpha_{13}$, and $G\alpha_q$.

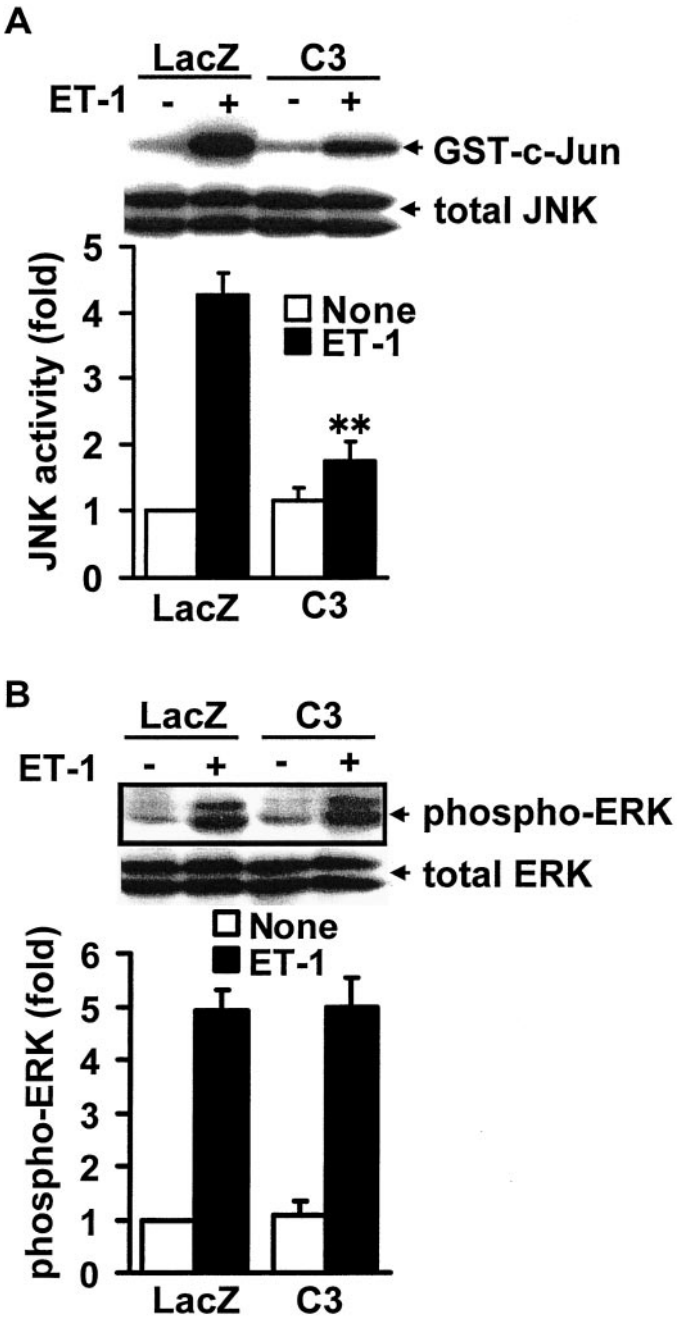

Fig. 10. Effects of C3 toxin on ET-1-induced activation of JNK and ERK. Cells expressing LacZ or C3 toxin were stimulated by ET-1, and JNK (A) and ERK activation (B) were determined as described under *Materials and Methods*. JNK and ERK activations are expressed as fold increase relative to those of unstimulated LacZ-expressing cells. A representative result is shown (top). Western blot of JNK or ERK using a portion of cell lysates revealed nearly equal amounts of JNK or ERK were used for immunoprecipitation (bottom). The result is shown as mean ± S.E. of three independent experiments (graph). **, $p < 0.01$ versus ET-1 stimulation of LacZ-expressing cells.

Acknowledgments

We are grateful to Dr. Dario Diviani for critically revising the manuscript. We thank Dr. Shuh Narumiya for C3 toxin plasmid, Drs. Tong-Chuan He and Bert Vogelstein for generously providing pAdEasy system, Dr. Melvin Simon for $G\alpha_{12}$ and $G\alpha_{13}$ plasmids, and Drs. Robert J. Lefkowitz for rat GRK2 plasmid and Hiroshi Nishina for GST-c-Jun plasmid. We also thank RIKEN DNA Bank for providing recombinant adenovirus of LacZ.

References

Akhter SA, Luttrell LM, Rockman HA, Iaccarino G, Lefkowitz RJ, and Koch WJ (1998) Targeting the receptor-G_q interface to inhibit in vivo pressure overload myocardial hypertrophy. *Science (Wash DC)* **280:**574–577.

Berestetskaya YV, Faure MP, Ichijo H, and Voyno-Yasenetskaya TA (1998) Regulation of apoptosis by α-subunits of G_{12} and G_{13} proteins via apoptosis signal-regulating kinase-1. *J Biol Chem* **273:**27816–27823.

Buhl AM, Johnson NL, Dhanasekaran N, and Johnson GL (1995) $G\alpha_{12}$ and $G\alpha_{13}$ stimulate Rho-dependent stress fiber formation and focal adhesion assembly. *J Biol Chem* **270:**24631–24634.

Carman CV, Parent JL, Day PW, Pronin AN, Sternweis PM, Wedegaertner PB, Gilman AG, Benovic JL, and Kozasa T (1999) Selective regulation of $G\alpha_{q/11}$ by an RGS domain in the G protein-coupled receptor kinase, GRK2. *J Biol Chem* **274:**34483–34492.

Collins LR, Minden A, Karin M, and Brown JH (1996) $G\alpha_{12}$ stimulates c-Jun NH_2-terminal kinase through the small G proteins Ras and Rac. *J Biol Chem* **271:**17349–17353.

De Vries L, Zheng B, Fischer T, Elenko E, and Farquhar MG (2000) The regulator of G protein signaling family. *Annu Rev Pharmacol Toxicol* **40:**235–271.

Gilchrist A, Vanhauwe JF, Li A, Thomas TO, Voyno-Yasenetskaya T, and Hamm HE (2001) Gα minigenes expressing C-terminal peptides serve as specific inhibitors of thrombin-mediated endothelial activation. *J Biol Chem* **276:**25672–25679.

Gohla A, Offermanns S, Wilkie TM, and Schultz G (1999) Differential involvement of $G\alpha_{12}$ and $G\alpha_{13}$ in receptor-mediated stress fiber formation. *J Biol Chem* **274:**17901–17907.

Hamm HE (1998) The many faces of G protein signaling. *J Biol Chem* **273:**669–672.
Hara Y, Wakamori M, Ishii M, Maeno E, Nishida M, Yoshida T, Yamada H, Shimizu S, Mori E, Kudoh J, et al. (2002) LTRPC2 Ca^{2+}-permeable channel activated by changes in redox status confers susceptibility to cell death. *Mol Cell* **9:**163–173.
Hart MJ, Jiang X, Kozasa T, Roscoe W, Singer WD, Gilman AG, Sternweis PC, and Bollag G (1998) Direct simulation of the guanine nucleotide exchange activity of p115 RhoGEF by $G\alpha_{13}$. *Science (Wash DC)* **280:**2112–2114.
He T-C, Zhou S, da Costa LT, Yu J, Kinzler KW, and Vogelstein BA (1998) Simplified system for generating recombinant adenoviruses. *Proc Natl Acad Sci USA* **95:** 2509–2514.
Hines WA and Thorburn A (1998) Ras and Rho are required for $G\alpha_q$-induced hypertrophic gene expression in neonatal rat cardiac myocytes. *J Mol Cell Cardiol* **30:**485–494.
Hoshijima M, Sah VP, Wang Y, Chien KR, and Brown JH (1998) The low molecular weight GTPase Rho regulates myofibril formation and organization in neonatal rat ventricular myocytes: involvement of Rho kinase. *J Biol Chem* **273:**7725–7730.
Kozasa T, Jiang X, Hart MJ, Sternweis PM, Singer WD, Gilman AG, Bollag G, and Sternweis PC (1998) p115 RhoGEF, a GTPase activating protein for $G\alpha_{12}$ and $G\alpha_{13}$. *Science (Wash DC)* **280:**2109–2111.
Kranenburg O, Poland M, van Horck FP, Drechsel D, Hall A, and Moolenaar WH (1999) Activation of RhoA by lysophosphatidic acid and $G\alpha_{12/13}$ subunits in neuronal cells: induction of neurite retraction. *Mol Biol Cell* **10:**1851–1857.
MacKinnon AC, Waters C, Jodrell D, Haslett C, and Sethi T (2001) Bombesin and substance P analogues differentially regulate G-protein coupling to the bombesin receptor. Direct evidence for biased agonism. *J Biol Chem* **276:**28083–28091.
Mehta D, Rahman A, and Malik AB (2001) Protein kinase C-α signals Rho-guanine nucleotide dissociation inhibitor phosphorylation and Rho activation and regulates the endothelial cell barrier function. *J Biol Chem* **276:**22614–22620.
Miyauchi T and Masaki T (1999) Pathophysiology of endothelin in the cardiovascular system. *Annu Rev Physiol* **61:**391–415.
Nishida M, Maruyama Y, Tanaka R, Kontani K, Nagao T, and Kurose H (2000) $G\alpha_i$ and $G\alpha_o$ are target proteins of reactive oxygen species. *Nature (Lond)* **408:**492–495.
Nishida M, Nagao T, and Kurose H (1999) Activation of Rac1 increases c-Jun NH_2-terminal kinase activity and DNA fragmentation in a calcium-dependent manner in rat myoblast cell line H9c2. *Biochem Biophys Res Commun* **262:**350–354.
Rümenapp U, Asmus M, Schablowski H, Woznicki M, Han L, Jakobs KH, Fahimi-Vahidi M, Michalek C, Wieland T, and Schmidt M (2001) The M3 muscarinic acetylcholine receptor expressed in HEK-293 cells signals to phospholipase D via G_{12} but not G_q-type G proteins: regulators of G proteins as tools to dissect pertussis toxin-resistant G proteins in receptor-effector coupling. *J Biol Chem* **276:**2474–2479.
Sah VP, Hoshijima M, Chien KR, and Brown JH (1996) Rho is required for $G\alpha_q$ and α_1-adrenergic receptor signaling in cardiomyocytes: dissociation of Ras and Rho pathways. *J Biol Chem* **271:**31185–31190.
Sakai S, Miyauchi T, Kobayashi M, Yamauchi I, Goto K, and Sugishita Y (1996) Inhibition of myocardial pathway improves long-term survival in heart failure. *Nature (Lond)* **384:**353–355.
Shubeita HE, McDonough PM, Harris AN, Knowlton KU, Glembotski C, Brown JH, and Chien KR (1990) Endothelin induction of inositol phospholipids hydrolysis, sarcomere assembly and cardiac gene expression in ventricular myocytes. A paracrine mechanism for myocardial cell hypertrophy. *J Biol Chem* **265:**20555–20562.
Simon MI, Strathmann MP, and Gautam N (1991) Diversity of G proteins in signal transduction. *Science (Wash DC)* **252:**802–808.
Sugden PH and Clerk A (1998) "Stress-responsive" mitogen-activated protein kinases (c-Jun N-terminal kinases and p38 mitogen-activated protein kinases) in the myocardium. *Circ Res* **83:**345–352.
Thorburn J, Xu S, and Thorburn A (1997) MAP kinase- and Rho-dependent signals interact to regulate gene expression but not actin morphology in cardiac muscle cells. *EMBO J* **16:**1888–1900.
Vilardaga J-P, Frank M, Krasel C, Dees C, Nissenson RA, and Lohse MJ (2001) Differential conformational requirements for activation of G proteins and the regulatory proteins arrestin and G protein-coupled receptor kinase in the G protein-coupled receptor for parathyroid hormone (PTH)/PTH-related protein. *J Biol Chem* **276:**33435–33443.
Voyno-Yasenetskaya T, Conklin BR, Gilbert RL, Hooley R, Bourne HR, and Barber DL (1994) $G\alpha_{13}$ stimulates Na-H exchange. *J Biol Chem* **269:**4721–4724.
Widmann C, Gibson S, Jarpe MB, and Johnson GL (1999) Mitogen-activated protein kinase: conservation of a three-kinase module from yeast to human. *Physiol Rev* **79:**143–180.
Yan Y, Chi PP, and Bourne HR (1997) RGS4 inhibits Gq-mediated activation of mitogen-activated protein kinase and phosphoinositide synthesis. *J Biol Chem* **272:**11924–11927.
Yuan J, Slice LW, and Rozengurt E (2001) Activation of protein kinase D by signaling through Rho and the α subunit of the heterotrimeric G protein G_{13}. *J Biol Chem* **276:**38619–38627.

Address correspondence to: Hitoshi Kurose, Department of Pharmacology and Toxicology, Graduate School of Pharmaceutical Sciences, Kyushu University, 3-1-1 Maidashi, Higashi-ku, Fukuoka 812-8582. E-mail: kurose@phar.kyushu-u.ac.jp